

Clustering of Ions at Atomic-Dimensions in Quantum Plasmas

P. K. Shukla^{1,2} and B. Eliasson¹

¹*International Centre for Advances Studies in Physical Sciences & Institute for Theoretical Physics, Faculty of Physics & Astronomy, Ruhr-University Bochum, D-44780 Bochum, Germany*

²*Department of Mechanical and Aerospace Engineering & Center for Energy Research, University of California San Diego, La Jolla, CA 92093, U. S. A.**

(Received 5 September 2012)

By means of particle simulations of the equations of motion for ions interacting with the newly discovered Shukla-Eliasson (SE) force in a dense quantum plasma, we demonstrate that the SE force is powerful to bring ions closer at atomic dimensions. Specifically, we present simulation results on the dynamics of an ensemble of ions in the presence of the SE force without and with confining external potentials and collisions between the ions and degenerate electrons. Our particle simulations reveal that under the SE force, ions attract each other, come closer and form ionic clusters in the bath of degenerate electrons that shield the ions. Furthermore, an external confining potential produces robust ion clusters that can have cigar-like and ball-like shapes. The binding between the ions on account of the SE force may provide possibility of non-Coulombic explosions of ionic clusters for inertial confined fusion (ICF) schemes when high-energy density plasmas (density exceeding 10^{23} per cubic centimeters) are produced by intense laser and relativistic electron beams. At such high plasma densities, the electrons will be degenerate and quantum forces due to the electron recoil effect caused by the overlapping of electron wavefunctions and electron tunneling through the Bohm potential, electron-exchange and electron correlations associated with electron-1/2 spin effect, and the quantum statistical pressure due to the Fermionic nature of degenerate electrons play a decisive role in producing the novel phenomena we describe in this paper.

PACS numbers: 71.10.Ca, 63.10.+a, 67.10.Hk

I. INTRODUCTION

During the early thirties, there were several discoveries related with non-Coulombic shielded potential distributions that exhibit the role of collective interactions between electrons and ions in electro-chemistry [1] (viz. electrolytes and colloidal suspensions), in solid state [2] and gaseous [3] plasmas, and neutrons and protons in elementary particle physics [4]. The screened non-Coulombic potentials, which were obtained by using the linearized theory based on the assumption that the potential energy between the particles is much smaller than the particle kinetic energy, are now known as the Debye-Hückel (DH), Thomas-Fermi (TF), and Yukawa potentials in the context of electro-chemistry and plasma physics, condensed matter physics, and nuclear physics, respectively. The well-celebrated DH, TF, and Yukawa potentials describe short-range (of the order of the DH radius, the TF radius, and the Yukawa radius, which are fixed by the size of a shielded cloud) repulsive interactions between two particles that have the same polarity. The DH theory has also been extended to the soft condensed matter physics of charged dust particles which are shielded by non-degenerate electrons and ions. The DH, TF, and Yukawa interaction potentials, which significantly deviate from the Coulomb interaction potential, have wide ranging applications with regard to

understanding phase transitions [5] in different areas of physical sciences that are at the cross-road of interdisciplinary subjects sharing knowledge.

In order for charged particles to form ordered structures under the influence of Coulombic, DH, TF and Yukawa repulsive forces, one must confine like charged particles in an external potential, so as to bring them to a minimum energy state. Examples include the Wigner crystals [6] composed of an ensemble of electrons on the surface of liquid helium, ion crystals in laser cooled Paul [7] and Penning (electromagnetic) traps [8], charged dust particle crystals [9], which were formed when like-charged particles were kept together via external confining potentials despite the short-range Coulombic or shielded Coulombic repulsive forces between charged particles. In fact, both electron and ion crystals, as well as crystals of colloidal suspensions and oil droplets have been observed experimentally under different environments [7, 8, 10, 12–17]. Moreover, an ensemble of strongly correlated micron-sized negative dust particles formed dust Coulomb crystals [18, 19] when they were confined by the sheath parabolic potential in low-temperature laboratory dusty plasma discharges [20]. The condensation of charged dust particles occurs since the dusty plasma Γ_d (the ratio between the Coulomb energy between highly charged dust grains and the dust particle kinetic energy) becomes relatively large due to the high dust charge state and low dust temperature. The attraction between like-charged dust particles forming dust Coulomb crystals may be attributed to attractive forces arising from overlapping of the dusty plasma Debye spheres [21], ion focusing and wakefield [22], and dipole-dipole interac-

*Electronic address: profshukla@yahoo.de

tions [19, 20]. The Cooper's pairing of charged dust particles, which are glued by ions, led to the discovery of a soft- condensed matter of dust particle crystals in low-density and low-temperature classical plasma with Maxwell-Boltzmann distributions for the plasma particles. It turns out that several milestones were put in the areas of ordered crystalline structures composed of charged particles (e.g. an ensemble of in low-temperature physical systems electrons, ions, as well as charged colloidal and dust particles) in physical systems which share some common physics.

However, at solid densities that are relevant for industrial applications (e.g. semiconductors and metallic nanostructures for thin films), as well as for compressed high-energy density (HED) plasmas produced by intense laser and relativistic electron beams for inertial confinement fusion (ICF) schemes, and for compact astrophysical objects (e.g white dwarf stars, warm dense matter) that are fundamental importance in astrophysics, one must account for degeneracy [23] of the electrons which obey the Fermi-Dirac distribution function. Subsequently, in HED plasmas, quantum mechanical effects play a vital role because in such plasmas the Wigner-Seitz radius $d = (3/4\pi n_0)^{1/3}$ is comparable to the thermal de Broglie wavelength $\lambda_B = \hbar/mV_T$, where \hbar is Planck's constant divided by 2π , m the electron mass, $V_T = \sqrt{k_B T/m}$ the electron thermal speed due to random motions of electrons, and k_B the Boltzmann constant. Also, in dense quantum plasmas with degenerate electrons, λ_B turns out to be much smaller than the Landau length $\lambda_L = e^2/k_B T$, which can be conveniently expressed as $k_B T \ll e^2/a_B$, where $a_B = \hbar^2/me^2$ is the Bohr radius of a hydrogen atom. The electron degeneracy effects at nanoscales in HED plasmas can only be captured through the consideration of the Fermi-Dirac statistics for electrons with spin-1/2 (Fermions), and overlapping of electron wavefunctions due to Heisenberg's uncertainty principle and Pauli's exclusion principle, as well as electron-exchange and electron-correlations due to electron spin-1/2. Thus, there are quantum forces [23, 24, 26–37] associated with the quantum statistical electron pressure [23–25], the quantum Bohm potential [26–28, 34, 35] through which degenerate electrons can tunnel through, as well as the electron-exchange and electron-correlations potentials [30, 38]. It has been found that the above mentioned quantum forces acting on degenerate electron fluids in quantum plasmas introduce new dispersive features to electron plasma oscillations [39, 40] with frequencies in the x-ray regime, which can be assessed by using collective x-ray spectroscopic scattering techniques [41, 42]. In fact, Glenzer *et al.* [41] have reported observations of electron plasma oscillations (EPOs) in solid density plasmas (with the peak electron number density $\sim 3 \times 10^{23} \text{ cm}^{-3}$ and the equilibrium electron and ion temperatures of 12 eV ($\sim 1.5 \times 10^5$ degrees Kelvin), which is different from the electron Fermi temperature $T_F = (\hbar^2/2k_B m_e)(3\pi^2 n_0)^{2/3} \approx 1.7 \times 10^5$ degrees Kelvin). Thus, the recent experiments of Glenzer

et al. [41] have unambiguously demonstrated the importance of the quantum statistical pressure and quantum electron recoil effects on the frequency spectra of EPOs [34, 39, 40], although a previous experimental investigation [43] has already examined the quantum properties of EPOs in metals.

Very recently, Shukla and Eliasson (SE) [44] have discovered an oscillating shielded Coulomb (OSC) potential, (also referred to as the SE attractive potential [45]), which is valid for the potential energy much smaller than $k_B T$ and mc^2 , around a stationary test ion in an unmagnetized quantum plasma due to collective interactions between an ensemble of degenerate electrons that shield ions at atomic dimensions, where c is the speed of light in vacuum. The profile of the OSC potential in quantum plasmas resembles the Lennard-Jones (LJ) potential in atomic gases. Hence, we have a novel attractive SE force (minus gradient of the OSC potential) that can bring ions closer to form ion clusters in high-energy density (HED) quantum plasmas. In this paper, we demonstrate the formation of ion clusters at atomic dimensions by performing computer simulations of the equations of motion for an ensemble of ions that are interacting with each other through the SE attractive force.

II. THE SE ATTRACTIVE FORCE

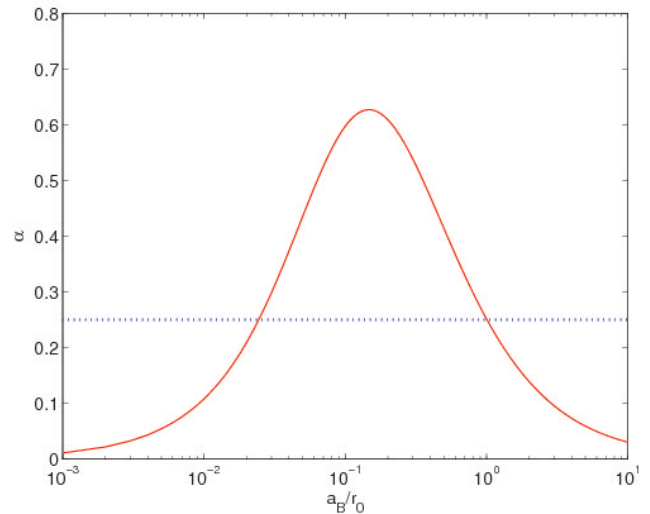


FIG. 1: The value of α as a function of a_B/r_0 . The critical value $\alpha = 1/4$ is indicated with a dotted line.

The existence of the SE attractive potential, which is obtained from Fourier transformation of Poisson's equation with the quasi-stationary electron density perturbation deduced from the linearized continuity and generalized momentum equation [44] for non-relativistic, degenerate electrons in a dense quantum plasma, critically depends on the electron number density through the parameter $\alpha = \hbar^2 \omega_{pe}^2 / 4m^2 u_*^4$,

where $u_* = (v_*^2/3 + v_{ex}^2)^{1/2}$. The parameter α measures the quantum recoil effect due to the quantum Bohm potential [26–28] $V_B = (\hbar^2/2m)(1/\sqrt{n})\nabla^2\sqrt{n}$ compared to the quantum statistical Fermi electron pressure and the electron-exchange and electron-correlations effects arising from 1/2-spin of degenerate electrons. Here $v_* = \hbar(3\pi^2)^{1/3}/mr_0$ is the electron Fermi speed and $v_{ex} = (0.328e^2/mr_0)^{1/2}[1 + 0.62/(1 + 18.36a_B n_0^{1/3})]^{1/2}$ includes the effects of electron exchange and electron correlations, where $r_0 = n_0^{-1/3}$ represents the average inter-electron distance. The expression for v_{ex} is derived by linearizing the sum of the electron exchange and electron correlation potentials [38] $V_{xc} = 0.985e^2 n^{1/3} [1 + (0.034/a_B n^{1/3})\ln(1 + 18.37a_B n^{1/3})]$. We note that α depends only on a_B/r_0 , as $\alpha = 9.3\pi(a_B/r_0)/[1 + (3\pi^2)^{2/3}(a_B/r_0) + 0.62/(1 + 18.36a_B/r_0)]^2$. Shukla and Eliasson [44] found that attractive potentials between ions exist only for $\alpha > 1/4$. Figure 1 displays the value of α as a function of a_B/r_0 , where one observes that it is above a critical value 0.25 only for a limited range $2 \times 10^{-2} < a_B/r_0 < 1$, corresponding to an electron number density in the range $5.4 \times 10^{19} \text{ cm}^{-3} < n_0 < 6.7 \times 10^{24} \text{ cm}^{-3}$ (with $a_B = 5.3 \times 10^{-9} \text{ cm}$). The maximum value is $\alpha \approx 0.627$ at $a_B/r_0 \approx 0.15$, corresponding to the electron number density $n_0 \approx 2 \times 10^{22} \text{ cm}^{-3}$, a few times below solid densities. The validity of the SE-OSC potential has been further expanded [45] for wider density ranges by including Chandrasekhar’s generalized pressure law [23] for degenerate electron fluids and Salpeter’s [46] electron-exchange and electron-correlations potentials that are of astrophysical interest.

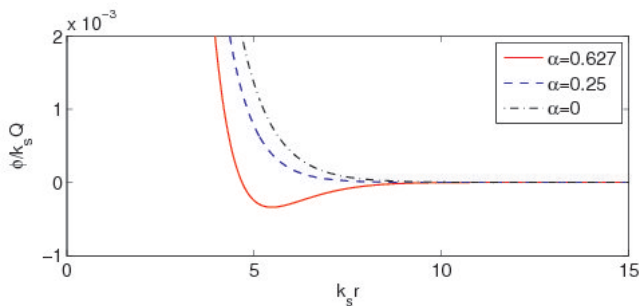


FIG. 2: (Color online) The electric potential ϕ as a function of r for $\alpha = 0.627$ (solid curve), $\alpha = 0.25$ (dashed curve) and $\alpha = 0$ (dash-dotted curve). The value 0.627 is the maximum possible value of α in our model, obtained for $a_B/r_0 \approx 0.15$.

For $\alpha > 0.25$, the profile of the electric potential as a function of distance r around a stationary test ion charge Q is [44]

$$\phi(\mathbf{r}) = \frac{Q}{r} [\cos(k_i r) + b_* \sin(k_i r)] \exp(-k_r r), \quad (1)$$

which is referred to as an oscillating Coulomb-screened (OCS) or the SE attractive potential. Here Q is the ion charge, $b_* = 1/\sqrt{4\alpha - 1}$, $k_i = (k_s/\sqrt{4\alpha})(\sqrt{4\alpha} - 1)^{1/2}$,

and $k_r = (k_s/\sqrt{4\alpha})(\sqrt{4\alpha} + 1)^{1/2}$, with $k_s = \omega_{pe}/u_*$ being the modified inverse TF screening length. We depict the potential in Fig. 2 which exhibits that it has a distinct minimum for $\alpha = 0.627$ that resembles the LJ potential. The negative part of the SE potential, given by Eq. (1), corresponds to a short-range SE attractive force (minus gradient of the SE potential) between ions. On the other hand, the potential distribution around a test ion for $\alpha < 0.25$ reads [44]

$$\phi(\mathbf{r}) = \frac{Q}{2r} [(1 + b) \exp(-k_+ r) + (1 - b) \exp(-k_- r)], \quad (2)$$

where $b = 1/\sqrt{1 - 4\alpha}$, and $k_{\pm} = k_s(1 \mp \sqrt{1 - 4\alpha})^{1/2}/\sqrt{2\alpha}$. For $\alpha \leq 0.25$, the potential is positive and monotonically decreasing (cf. Fig. 2), giving rise to only a repulsive force (similar to the TF force) between ions. In the high- or low-density limit, where $\alpha \rightarrow 0$, we recover the modified TF screened Coulomb potential $\phi(\mathbf{r}) = (Q/r) \exp(-k_s r)$.

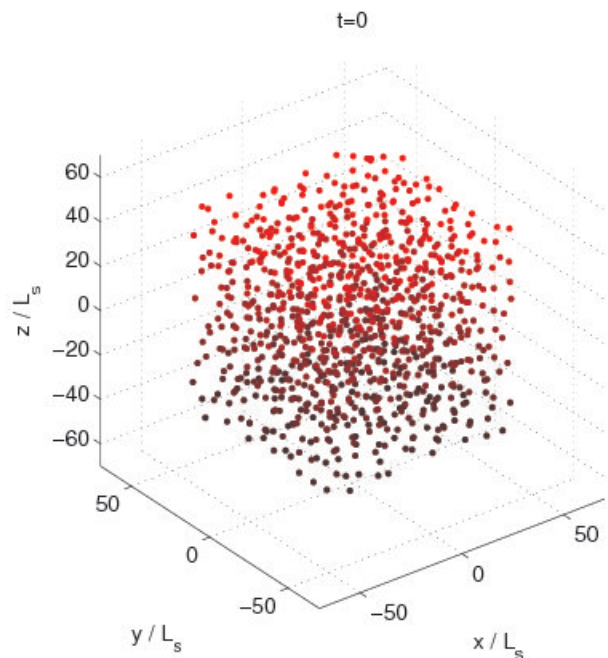


FIG. 3: (Color online) The initial positions of ions in the particle simulations.

III. DEMONSTRATION OF ION CLUSTERING

We present a computer simulation study of the dynamics of a system of ions interacting with each other under the action of the SE attractive force. For our purposes, we numerically solve the equations of motion for a system of ions with equal charges and masses, given by

$$M \frac{d\mathbf{v}_j}{dt} = -Q \sum_{i \neq j} \nabla_j \phi(|\mathbf{R}_{ij}|) - \nabla_j V_c(\mathbf{r}_j) - M\nu \mathbf{v}_j, \quad (3)$$

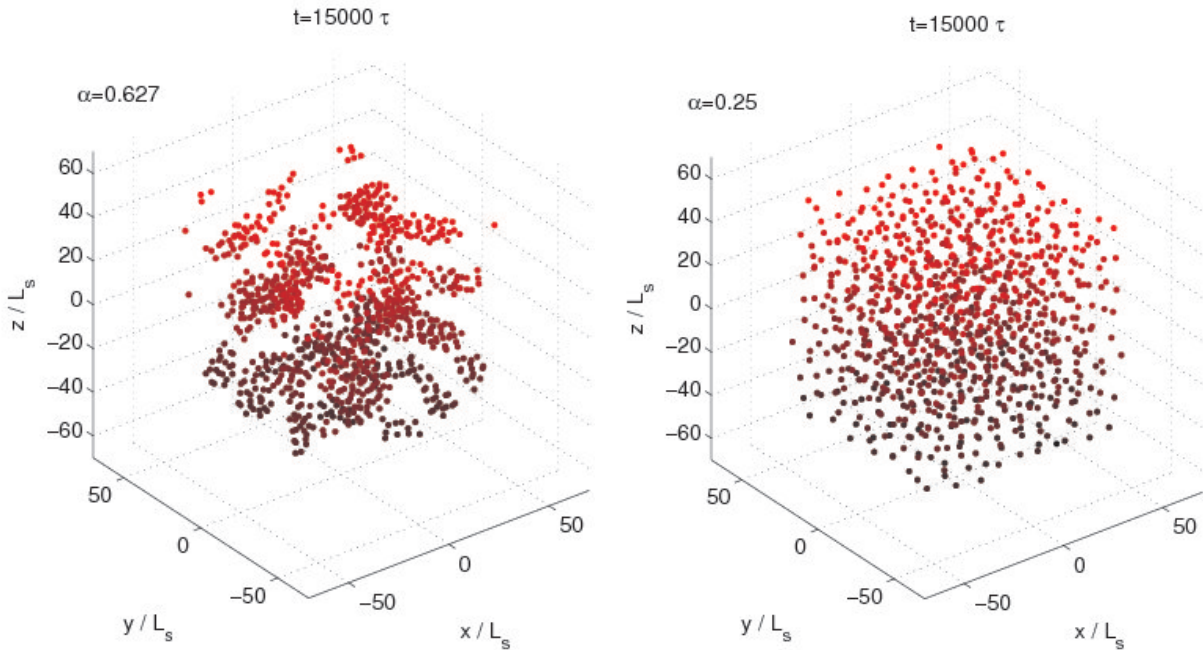


FIG. 4: (Color online) The positions of ions at $t = 15000 \tau$ for $\alpha = 0.627$ (left) and $\alpha = 0.25$ (right), showing the clustering and solidification of the ions for $\alpha = 0.627$, but not for $\alpha = 0.25$.

where instantaneous position of ions is determined from $d\mathbf{r}_j/dt = \mathbf{v}_j$. Here $\mathbf{R}_{ij} = \mathbf{r}_i - \mathbf{r}_j$ is the radius vector between particle i and j , $\mathbf{r}_j(t)$ the position and $\mathbf{v}_j(t)$ the velocity of the j th ion, M the mass of the ion (∇_j denotes the gradient of ϕ at position \mathbf{r}_j), and ν denotes an effective ion collision frequency, which tends to retard the ion motions. The external confining potential, $V_c(\mathbf{r}) = (M/2)(\omega_\perp^2 r_\perp^2 + \omega_z^2 z^2)$, of charged particles may have different amplitudes ω_\perp and ω_z perpendicular and parallel to the z -axis, respectively, where $r_\perp^2 = r_x^2 + r_y^2$.

In order to demonstrate clustering of ions under the SE attractive force, we now carry out particle simulations of Eq. (3) with 1000 particles, initially randomly placed in space as shown in Fig. 3. In the first set of simulations, displayed in Fig. 4, we consider interactions of ions in the absence of the external confining potential V_c , viz. $\omega_z = \omega_\perp = 0$, and with $\nu = 0.01 \tau^{-1}$. The positions of ions at the end of the simulation are shown in Fig. 4 at time $t = 15000 \tau$. Here the positions and time are in units of $L_s = k_s^{-1}$ and $\tau = M^{1/2}/Qk_s^{3/2} = (\pi/16)^{1/8}(a_B/r_0)^{3/8}\omega_{pi}^{-1}/\alpha^{3/8}Z_i$, respectively, where $\omega_{pi} = (4\pi Q^2 n_{i0}/M)^{1/2}$ is the ion plasma frequency, and n_{i0} is the equilibrium ion number density, related to the electron number density n_0 via the quasi-neutrality condition $Z_i n_{i0} = n_0$, where Z_i is the ion charge state. For $\alpha = 0.627$, which leads to a potential minimum (cf. Fig. 2), we observe the clustering of ions and the formation of large scale ionic structures. The clustering of ions is a relatively slow process in comparison with the ion plasma period $2\pi/\omega_{pi}$. Ion pairs and smaller clusters are initially formed, and later

the larger ion clusters are gradually formed by the agglomeration of smaller ion clusters. We can estimate the coagulation temperature T_{ic} for ions from the relation $k_B T_{ic} = Q\phi_{min}$, where ϕ_{min} is the magnitude of the potential minimum around the test charge $Q = Z_i e$. If we denote $\varphi_{min} = \phi_{min}/k_s Q$; we note from Fig. 2 that $\varphi_{min} \approx 3 \times 10^{-4}$ for $\alpha = 0.627$. Using the expression for α , we then obtain the coagulation temperature from $k_B T_{ic} = 2\pi^{1/4}(Q^2/r_0)\varphi_{min}(\alpha r_0/a_B)^{1/4}$, where one has to deduce α for given values of a_0/r_0 from Fig. 1. For a hydrogen ion with $a_0/r_0 = 0.15$ and $\alpha = 0.627$, we find that $\varphi_{min} = 3 \times 10^{-4}$ and $T_{ic} = 54$ K. As a contrast, for $\alpha = 0.25$, we see in Fig. 4 that there does not exist condensation/coalescence of ions. This is due to the fact that there is no potential minimum for this value of α (cf. Fig. 2), and hence the inter-ion force is always repulsive.

Furthermore, we have carried out a set of simulations with a symmetric potential V_c with $\omega_\perp = \omega_z = 2 \times 10^{-3} \tau^{-1}$. Here, as seen in Fig. 5, almost spherical non-Coulomb ion crystals are formed for both $\alpha = 0.627$ and $\alpha = 0.25$. Finally, we have performed simulations including an asymmetric external potential V_c with $\omega_\perp = 6 \times 10^{-3} \tau^{-1}$ and $\omega_z = 2 \times 10^{-3} \tau^{-1}$, providing a stronger confinement in the perpendicular direction. Figure 6 displays the final state for $\alpha = 0.627$ and $\alpha = 0.25$, where ions, in both cases, form non-Coulombic ion crystals elongated along the z -direction. In general, the formation of non-Coulombic ion crystals is attributed to the balance between the external and inter-ion potentials, where the system tends to a configuration of a minimum potential energy. We note that similar configura-

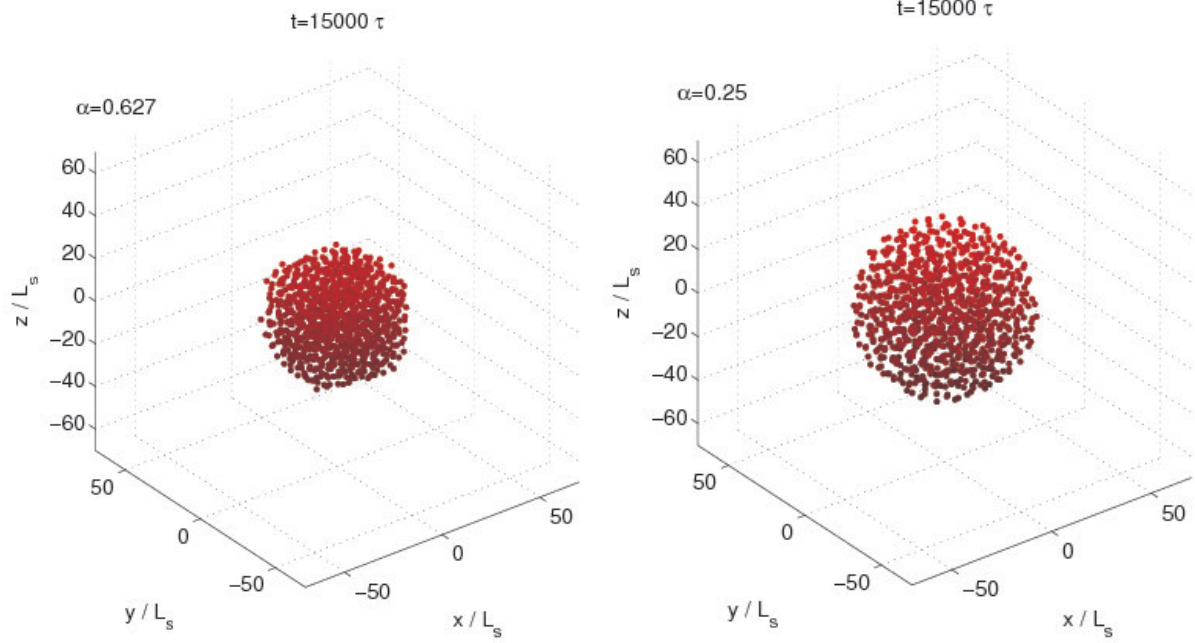


FIG. 5: (Color online) The positions of ions at $t = 15000$ for $\alpha = 0.627$ (left) and $\alpha = 0.25$ (right) including a symmetric parabolic potential with $\omega_{\perp} = \omega_z = 2 \times 10^{-3} \tau^{-1}$, leading to the formation of almost spherical non-Coulombic ion crystals.

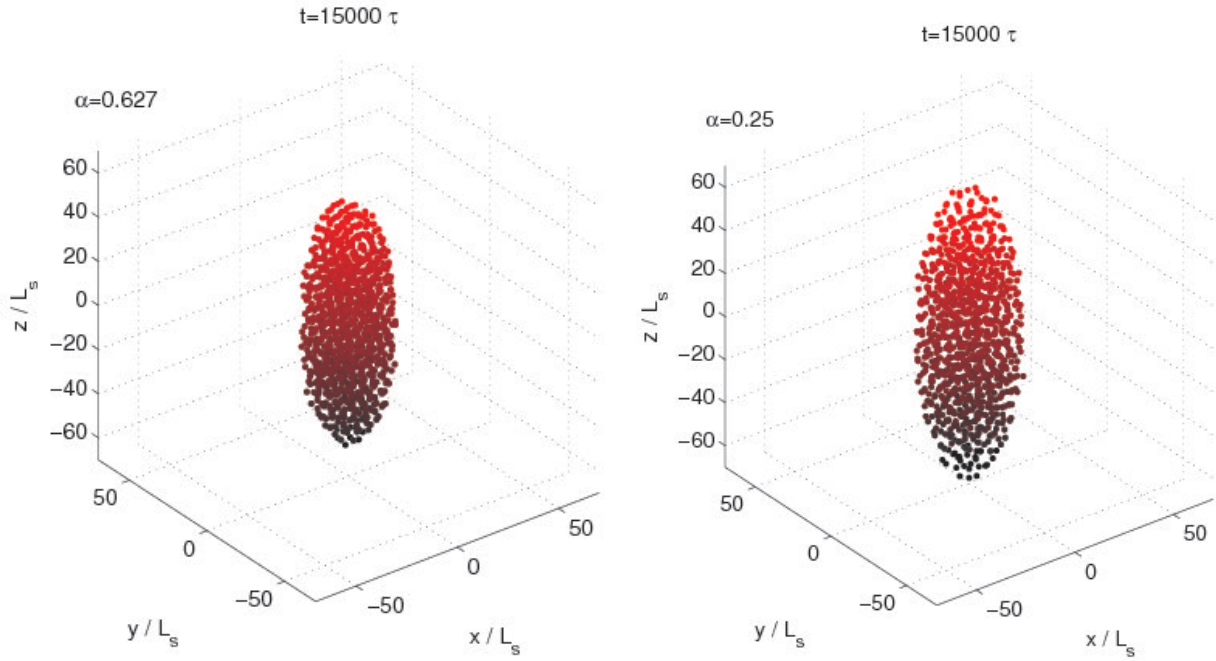


FIG. 6: (Color online) The positions of ions at $t = 15000$ for $\alpha = 0.627$ (left) and $\alpha = 0.25$ (right) including parabolic potential with $\omega_{\perp} = 6 \times 10^{-3} \tau^{-1}$ and $\omega_z = 2 \times 10^{-3} \tau^{-1}$. Here elongated non-Coulombic ion crystals are formed.

rations have been previously reported for both charged macro-particles [9] and ions [7, 15, 17] confined by external potentials in the Paul trap. The formation of ion crystals can be detected by taking the spatial Fourier transform of the particle position, as shown in Fig. 7.

Initially, using the distribution of particles in Fig. 3, the spectrum in left-panel of Fig. 7 is uniform and no ordered ion structures can be detected. However, at the end of the simulation (using the result in left panel in Fig. 5), there are clear indications that ions have formed peri-

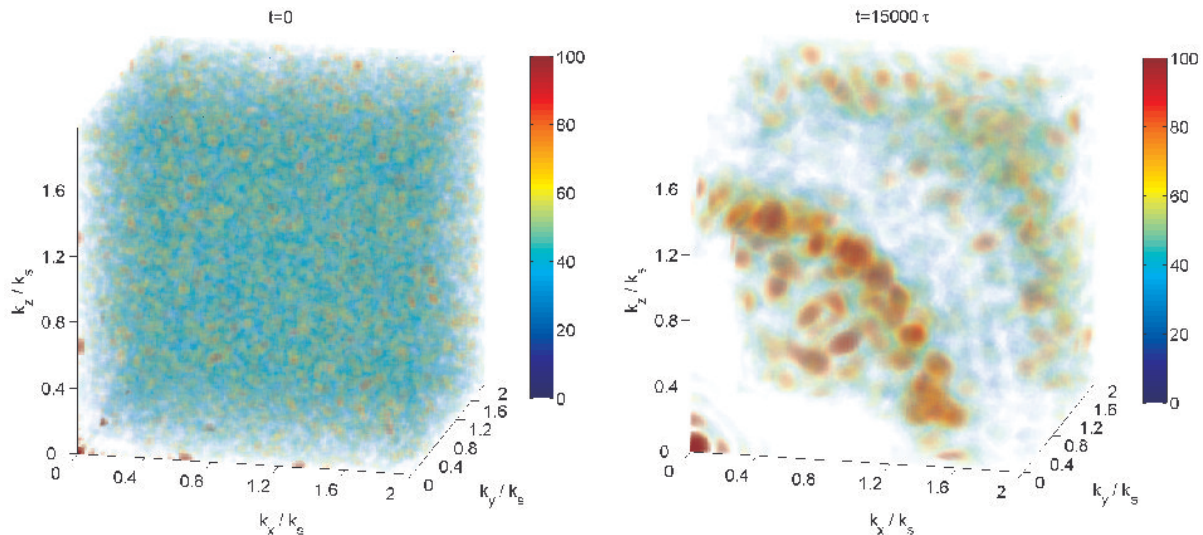


FIG. 7: (Color online) The Fourier transform of ion positions for (left) the initial condition in Fig. 3, and (right) for the spherical non-Coulombic ball with $\alpha = 0.627$ in Fig. 5. Initially the positions and the Fourier spectrum are random, but at the end of the simulation, Fourier components are concentrated at a spherical shell for wavenumbers $|\mathbf{k}| \approx 1.5 k_s$, indicating crystalline ion structures with an inter-ion distance $\approx 4k_s^{-1}$.

odic structures with a typical wavenumber of $\sim 1.5k_s$, indicating a periodic inter-ion distance of $\sim 4k_s^{-1}$.

IV. SUMMARY AND CONCLUSIONS

In summary, we have carried out particle simulations to demonstrate clustering of ions due to the newly found SE attractive force arising from collective interactions between an ensemble of degenerate electrons that shield ions in HED quantum plasmas. Specifically, the SE attractive force leads to clustering/condensation or coagulation of ions in the absence of an external confining potential for charged particles. We believe that the formation of ion clusters are going to play valuable roles in the area of compressed plasmas with degenerate electrons [42, 47, 48] for ICF to succeed, and also in the emerging field of nano-material sciences (e.g. nanodiodes, metallic nanostructures for thin films [30], nanowires, table-

top quantum free-electron- lasers [49–51] to be used as tunable coherent radiation sources for practical applications), where closely-packed ions will lend support to enhanced fusion probabilities (with anomalous fusion cross-sections) for controlled thermonuclear ICF, and may also influence the electric properties (e.g. resistivity) of new super-condensed plasma materials. Specifically, we stress that the Cooper pairing of ions at atomic dimensions shall provide possibility of novel superconducting plasma-based nanotechnology, since the electron transport in nanostructures would be rapid due to shortened distances between ions in the presence of the novel SE attractive force.

Acknowledgments

This work was supported by the Deutsche Forschungsgemeinschaft through the project SH21/3-2 of the Research Unit 1048.

-
- [1] P. Debye and E. Hückel, Phys. Z. **24**, No. 9, 185 (1923).
 - [2] L. H. Thomas, Math. Proc. Cambridge Phil. Soc. **23**, 542 (1927); E. Fermi, Rend. Acad. Na. Lincei **6**, 602 (1927).
 - [3] I. Langmuir, Phys. Rev. **33**, 954 (1929).
 - [4] H. Yukawa, Proc. Phys.-Math. Jpn. **17**, 48 (1935).
 - [5] K. Kremer, M. O. Robbins, and G. S. Grest, Phys. Rev. Lett. **57**, 2694 (1986); K. Avinash, *ibid.* **98**, 095003 (2007); B. Klumov, Phys. Usp. **53**, 1053 (2010).
 - [6] E. Wigner, Phys. Rev. **46**, 1002 (1934).
 - [7] M. Drewsen, C. Brodersen, L. Hornekær, J. S. Hangst, and J. P. Schiffer, Phys. Rev. Lett. **81**, 2878 (1998)
 - [8] J. N. Tan, J. J. Bollinger, B. Jelenkovic, and D. J. Wineland, Phys. Rev. Lett. **75**, 4198 (1995).
 - [9] R. F. Wuerker, H. Shelton, and R. V. Langmuir, J. Appl. Phys. **30**, 342 (1959).
 - [10] T. G. O. Berg and T. A. Gaukler, Am. J. Phys. **37**, 1013 (1969).
 - [11] R.S. Crandall and R. Williams, Phys. Lett. A **34**, 404 (1971).
 - [12] C. C. Grimes and G. Adams, Phys. Rev. Lett. **42**, 795 (1979).
 - [13] H. Winter and H. W. Ortjohann, Am J. Phys. **59**, 807 (1991).
 - [14] S. Robertson and R. Younger, Am. J. Phys. **67**, 310

- (1999).
- [15] K. Mølhave and M. Drewsen, Phys. Rev. A **62**, 011401 (2000).
- [16] V. V. Deshpande and M. Bockrath, Nature Physics **4**, 314 (2008).
- [17] Peter F. Staunum, Klaus Højbjerg, Peter S. Skyt, Anders K. Hansen and Michael Drewsen, Nature Phys. **6**, 271 (2010).
- [18] J. H. Chu and Lin I, Phys. Rev. Lett. **72**, 4009 (1994); H. Thomas, G. Morfill, and D. Demmel *et al.*, *ibid.* **73**, 652 (1994); Y. Hayashi and K. Tachibana, Jpn. J. Appl. Phys. **33**, L804 (1994).
- [19] U. Mohideen, H. U. Rahman, M. A. Smith, M. Rosenberg, and D. A. Mendis, Phys. Rev. Lett. **81**, 349 (1998).
- [20] P. K. Shukla and A. A. Mamun, *Introduction to Dusty Plasma Physics* (Institute of Physics, Bristol, 2002); P. K. Shukla and B. Eliasson, Rev. Mod. Phys. **81**, 25 (2009).
- [21] D. P. Resendes, J. T. Mendonça, and P. K. Shukla, Phys. Lett. A **239**, 181 (1998).
- [22] M. Nambu, S. V. Vladimirov, and P. K. Shukla, Phys. Lett. A **203**, 40 (1995); S. V. Vladimirov and M. Nambu, Phys. Rev. E **52**, R2172 (1995). P. K. Shukla and N. N. Rao, Phys. Plasmas **3**, 1770 (1996).
- [23] S. Chandrasekhar, Philos. Mag. **11** 992 (1931); Z. Astrophys. **5**, 321 (1932); Astrophys. J. **74**, 81 (1933); Mon. Not. R. Aston. Soc., **95** 207 (1935); *ibid.*, **96**, 644 (1936).
- [24] S. Chandrasekhar, *An Introduction to the Study of Stellar Structure* (The University of Chicago Press, Chicago, 1939).
- [25] L. D. Landau and E. M. Lifshitz, *Statistical Physics* (Butterworth-Heinemann, Oxford, 1980).
- [26] H. E. Wilhelm, Z. Phys. **241**, 1 (1971).
- [27] C. L. Gardner and C. Ringhofer, Phys. Rev. E **53**, 157 (1996).
- [28] G. Manfredi and F. Haas, Phys. Rev. B **64**, 075316 (2001); G. Manfredi, Fields Inst. Commun. **46**, 263 (2005).
- [29] P. K. Shukla and B. Eliasson, Phys. Rev. Lett. **96**, 245001 (2006); *ibid.* **99**, 096401 (2007); D. Shaikh and P. K. Shukla, *ibid.* **99**, 125002 (2007).
- [30] N. Crouseilles, P. A. Hervieux, and G. Manfredi, Phys. Rev. B **78**, 155412 (2008).
- [31] G. Brodin, M. Marklund, and G. Manfredi, Phys. Rev. Lett. **100** 175001 (2008).
- [32] D. B. Melrose, *Quantum Plasmadynamics: Unmagnetized Plasmas* (Springer, Berlin, 2008).
- [33] N. L. Tsintsadze and L. N. Tsintsadze, Europhys. Lett. **88**, 35001 (2009).
- [34] P. K. Shukla and B. Eliasson, Phys. Usp. **53** 51 (2010); Rev. Mod. Phys., **83** 885 (2011).
- [35] F. Haas, *Quantum Plasmas: An Hydrodynamical Approach* (Springer, New York, 2011).
- [36] S. V. Vladimirov and Yu. O. Tyshetskiy, Phys. Usp. **54** 1243 (2011).
- [37] J. T. Mendonça, Phys. Plasmas **18**, 062101 (2011).
- [38] L. Brey, J. Dempsey, N. F. Johnson, and B. I. Halperin, Phys. Rev. B. **42**, 1240 (1990); see also L. Hedin and B. I. Lundqvist, J. Phys. C: Solid State Phys. **4**, 2064 (1971).
- [39] Yu. L. Klimontovich and V. P. Silin, Dokl. Nauk SSR, **82** 361 (1952); Zh. Eksp. Teor. Fiz., **23** 151 (1952).
- [40] D. Bohm, Phys. Rev. **85** 166 (1952); D. Bohm and D. Pines, Phys. Rev. E, **92** 609 (1953).
- [41] S. H. Glenzer, O. L. Landen, P. Neumayer, R. W. Lee, K. Widmann, S. W. Pollaine, R. J. Wallace, G. Gregori, A. Holl, T. Bornath, R. Thiele, V. Schwarz, W. D. Kraeft, R. Redmer, Phys. Rev. Lett., **98** 065002 (2007).
- [42] S. H. Glenzer and R. Redmer, Rev. Mod. Phys. **81** 1625 (2009).
- [43] H. Watanabe, J. Phys. Soc. Jpn, **11** 112 (1956).
- [44] P. K. Shukla, B. Eliasson, Phys. Rev. Lett. **108** 165007 (2012); *ibid.*, **108** 219902(E) (2012); *ibid.* **109** 019901 (E) (2012).
- [45] M. Akbari-Moghanjoughi, J. Plasma Phys. **78**, Shukla-Eliasson Attractive Force: Revisited, in press, (2012); DOI: <http://dx.doi.org/S00223778120000839>; E-print: arXiv:1207.5154v2 [astro-ph.EP].
- [46] E. E. Salpeter, Astrophys. J. **134**, 669 (1961).
- [47] S. Son and N. J. Fisch, Phys. Rev. Lett. **95**, 225002 (2005); Phys. Lett. A **329**, 76 (2004); *ibid.* **356**, 65 (2006).
- [48] V. M. Malkin, N. J. Fisch, and J.S. Wurtele, Phys. Rev. E **75**, 026404 (2007).
- [49] Z. Huang and K.-J. Kim, Phys. Rev. ST Accel. Beams **10**, 034801 (2007).
- [50] A. Serbeto, L. F. Monteiro, K. H. Tsui, and J. T. Mendonça, Plasma Phys. Controlled Fusion **51**, 124024 (2009).
- [51] B. Eliasson and P. K. Shukla, Phys. Rev. E **85**, 065401(R) (2012).